Imaging-Based Surrogate Markers of Epidermal Growth Factor Receptor Mutation in Lung Adenocarcinoma

AlGharras, Abdulaziz; Kovacina, Bojan; Tian, Zhe; Alexander, James W.; Semionov, Alexandre; van Kempen, Leon C.; Sayegh, Karl

Published in:
Canadian association of radiologists journal-Journal de l association canadienne des radiologistes

DOI:
10.1177/0846537119888387

Publication date:
2020

Canadian Association of
Radiologists' Journal
1-9

DOI: 10.1177/0846537119888387
journals.sagepub.com/home/caj
SAGE

Imaging-Based Surrogate Markers of Epidermal Growth Factor Receptor Mutation in Lung Adenocarcinoma: A Local Perspective

Abdulaziz AlGharras, MD[1,2], Bojan Kovacina, MD[3], Zhe Tian, MSc[4], James W. Alexander, MD[1], Alexandre Semionov, MD[1], Léon C. van Kempen, MD[5,6], and Karl Sayegh, MD[1]

Abstract

Purpose: To identify computed tomography (CT) features of epidermal growth factor receptor (EGFR) mutation-positive lung adenocarcinoma in Canadian population and whether imaging-based surrogate markers of EGFR mutation in our population were similar to those found in the Asian population. **Materials and Methods:** Pretreatment CT scans of 223 patients with adenocarcinoma of the lung (112 with EGFR mutation and 111 without mutation) were retrospectively assessed for 20 specific CT features by 2 radiologists, who were blinded to the status of EGFR mutation. Univariate and multivariate logistic regression analyses as well as areas under the receiver operating characteristic curve were performed to discriminate characteristics of EGFR-activating mutation features. **Results:** Epidermal growth factor receptor mutation-positive adenocarcinomas were more frequently found in female ($P < .03$), less than 20 pack-year smoking history ($P < .001$), smaller tumor ($P < .01$), spiculated margins ($P < .05$), without centrilobular emphysema ($P < .001$), and without lymphadenopathy ($P < .05$), similarly to the Asian population. Multivariate logistic regression analyses of combined clinical and radiological features identified less than 20 pack-year smoking history, smaller tumor diameter, fine or coarse spiculations, noncentral location of the tumor, and lack of centrilobular emphysema and pleural attachment as the strongest independent prognostic factors for the presence of an EGFR mutation. These combined features improved prognostic ability area under the curve to 0.879, compared to 0.788 for clinical features only. **Conclusion:** Several CT findings may help predict the presence of an activating mutation in EGFR in lung adenocarcinomas in our Canadian population. Combining clinical and radiological features improves prognostic ability to determine the EGFR mutation status compared to clinical features alone.

Résumé

Objectif : Identifier les caractéristiques tomodensitométriques (TDM) de l'adénocarcinome pulmonaire positif pour la mutation du récepteur du facteur de croissance épidermique (*epidermal growth factor receptor*, EGFR) dans la population canadienne et déterminer si les marqueurs d'imagerie de substitution de la mutation de l'EGFR sont similaires à ceux décelés dans la population asiatique. **Matériel et méthodes :** Deux radiologistes ont réalisé une analyse rétrospective des clichés d'examen de TDM effectués avant traitement chez 223 patients présentant un adénocarcinome pulmonaire (112 avec mutation de l'EGFR et 111 sans cette mutation) en ciblant 20 caractéristiques de TDM spécifiques; cette analyse a été effectuée à l'aveugle en ce qui concerne le statut de la mutation de l'EGFR. Des analyses de régression logistique univariées et multivariées et les aires sous la courbe des caractéristiques de performance (ROC) ont été employées pour identifier les caractéristiques des signes de mutation activatrice de l'EGFR. **Résultats :** Les adénocarcinomes positifs pour la mutation du récepteur du facteur de croissance épidermique (EGFR) étaient plus fréquents chez les femmes ($P < 0,03$), avec des antécédents de tabagisme inférieur à 20 paquets par an ($P < 0,001$), en

[1] Department of Radiology, McGill University Health Center, Montreal, Quebec, Canada
[2] Department of Radiology, Unaizah College of Medicine, Qassim University, Qassim, Saudi Arabia
[3] Department of Radiology, Jewish General Hospital, Montreal, Quebec, Canada
[4] Cancer Prognostics and Health Outcomes Unit, University of Montreal Health Center, Montreal, Quebec, Canada
[5] Department of Pathology, McGill University and OPTILAB-McGill University Health Center, Montreal, Quebec General Hospital, Montreal, Quebec, Canada
[6] Department of Pathology, Laboratory for Molecular Pathology, University Medical Center Groningen, Groningen, the Netherlands

Corresponding Author:
Abdulaziz AlGharras, MD, Department of Radiology, McGill University Health Center, Montreal, Quebec, Canada H4A 3J1.
Email: abdulaziz.algharras@mail.mcgill.ca

présence d'une tumeur plus ténue (P < 0,01), en présence de marges à spicules (P < 05) et en l'absence d'emphysème centrolobulaire (P < 0,001) ou de lymphadénopathie (P < 0,05), de manière similaire à la population asiatique. Les analyses de régression logistique multivariées des signes cliniques et radiologiques combinés ont permis d'identifier les facteurs suivants comme étant les facteurs indépendants de pronostic de la présence de mutation de l'EGFR les plus importants : antécédents de tabagisme inférieur à 20 paquets par an, diamètre tumoral inférieur, spiculations fines ou épaisses, emplacement non central de la tumeur, et peu de présence d'emphysème centrolobulaire et d'adhérence pleurale. La combinaison de ces signes a entraîné une hausse de la capacité pronostique inhérente à l'aire sous la courbe de 0,879, par rapport à 0,788 pour les signes cliniques seuls. **Conclusion :** Plusieurs signes de TDM pourraient contribuer à prédire la présence d'une mutation activatrice de l'EGFR dans la population canadienne atteinte d'adénocarcinome pulmonaire. La combinaison des signes cliniques et radiologiques améliore la capacité pronostique du statut de mutation de l'EGFR par comparaison à l'utilisation des signes cliniques uniquement.

Keywords
EGFR mutation, lung adenocarcinoma, lung cancer in Canada, CT features, CT findings

Introduction

Epidermal growth factor receptor (EGFR) is a cell-surface protein, a tyrosine kinase, which activates cellular signaling pathways involved in regulation of cell growth, division, and differentiation. Activating mutation in the *EGFR* gene occurs in 8.5% to 27% of non-small cell lung carcinomas (NSCLC) and results in cell growth promoting activation of EGFR signaling.[1,2] The presence of an EGFR-activating mutation is strongly predictive of therapy response to anti-EGFR tyrosine kinase inhibitor (TKI) therapy.[3]

Epidermal growth factor receptor mutation is detected by DNA sequence analysis of the tumor cells from biopsy samples or pleural fluid and, more recently, in plasma.[4] Epidermal growth factor receptor mutation testing is currently the only approved test for selecting patients eligible for treatment with EGFR TKI. Although highly effective, the existing methods require an additional diagnostic step, thus increasing health-care costs. On the other hand, nearly all patients diagnosed with lung cancer nowadays undergo a diagnostic computed tomography (CT) of the chest to determine tumor burden. With that in mind, the identification of strong radiological features of NSCLC that perfectly correlate with EGFR mutation status could potentially be used to develop a CT image-based tool to predict the presence of an EGFR-activating mutation in the tumor.

A recent study conducted in China by Liu et al[5] has demonstrated an association between several radiological findings on CT and EGFR mutation status in 385 patients with lung adenocarcinoma. Their study lends some support to the idea of using tumor radiological features as surrogate marker for EGFR mutation detection. However, ethnicity-associated differences in the prevalence of EGFR mutations and distribution of mutation types have been described.[6] Thus, we set out to verify whether the results of Liu et al are applicable to a North American cohort of patients with lung cancer.

The primary objective of the current study is to identify CT features of EGFR mutation-positive lung adenocarcinoma in a heterogeneous, multiethnic, Canadian population. Our secondary objectives are to determine whether the imaging-based surrogate markers of EGFR mutation in a Canadian population were similar to those found in the Asian population and to establish whether CT features in combination with clinical variables could predict EGFR mutation status of lung adenocarcinoma.

Materials and Methods

Data Source and Setting

Our data were sourced from an academic tertiary care center serving a large metropolitan area in the province of Quebec, Canada. This retrospective study included patients with histopathologically confirmed adenocarcinoma of the lung diagnosed between January 2011 and October 2016. Tissue specimens were obtained by way of surgical resection, transthoracic needle biopsy, endobronchial ultrasound bronchoscopy, pleural fluid analysis, or tissue sampling of an extrapulmonary metastatic site. The results of the EGFR mutation status were obtained from a molecular genotyping registry of a previous study approved by the hospital's ethics committee. For our study, we have adopted the list of assessed radiological features from a previously published study of an Asian cohort.[5] A complete list of the CT features assessed in our study along with their definitions can be found in Table 1.

The following inclusion criteria were applied to the source data: available pathology report with a diagnosis of lung adenocarcinoma, available pretreatment thin-section CT images of the primary lung tumor, available EGFR mutation test result including the type of mutation, and available clinical information including age and sex. Among all the EGFR mutation-positive patients, after applying all the inclusion criteria, we retained a total of 112 patients. A comparison cohort of patients with non-EGFR-mutated adenocarcinomas (n = 112) was selected and matched for age and sex. At the analysis stage, 1 patient from the comparison cohort was removed due to lack of specific pathological diagnosis. Thus, a total of 223 patients were retained in our final analysis data set.

Computed Tomography Scanning Protocol

Multidetector CT scans of the chest, abdomen, and neck were used in this study to assess the original tumor. All scans of the

Table 1. List of Radiological Features Examined and Their Clinical Definition.

CT Features	Clinical Definition	Inter-Reader Agreement
Distribution	Tumor location in the lungs. Three zones are identified: central, mid, and peripheral.	$\kappa = 1$
Lobe location	Lobe location of the tumor.	$\kappa = 0.766$
Size; long axis	Long-axis diameter refers to the longest diameter of the tumor, measured in lung window setting.	ICC = 0.96
Size; short axis	Short-axis measurement of the tumor, perpendicular to long-axis diameter, measured in lung window setting.	ICC = 0.95
Shape	Overall shape of the tumor classified as: round, oval, or irregular.	$\kappa = 0.602$
Lobulation	Wavy or scalloped configuration of the tumor surface with at least 5-mm tissue thickness extending beyond the main contour of the tumor.	$\kappa = 0.766$
Borders	Borders can be well- or ill-defined. Ill-defined borders can be due to spiculated borders (fine or coarse) or obscured borders (when >25% of the border of the lesion is obscured).	$\kappa = 0.697$
Spiculation	Lines radiating from the margins of the tumor to the lung parenchyma but not extending to the pleural margin. Fine spiculations are defined as $\leq$2 mm long and coarse spiculations are defined as >2 mm long.	$\kappa = 0.540$
Texture	Tumor texture is classified as: pure ground glass, mixed attenuation/density, or solid.	$\kappa = 0.795$
Air bronchogram	Tube-like or branching air column within the tumor.	$\kappa = 0.728$
Air within the tumor	Presence of an air lucency within the tumor classified as bubbly air lucency or cavitation. Bubble like lucencies are defined as round-shaped air bubbles measuring $\leq$5 mm in diameter. Cavitation is defined as an air-containing cavity measuring >5 mm.	$\kappa = 0.677$
Pleural and fissural retraction	Retraction of the pleura or fissure toward the tumor or presence of a pleural tag originating from the edge of the tumor and extending peripherally to contact the pleural surface or fissure.	$\kappa = 0.627$
Peripheral emphysema	Perilesional emphysema caused by the tumor or preexisting centrilobular emphysema.	$\kappa = 0.897$
Peripheral fibrosis	Presence of perilesional fibrosis caused by the tumor or preexisting lung fibrosis.	$\kappa = 0.493$
Nodules in primary tumor lobe	Presence of noncalcified nodule suspected to be malignant or indeterminate in the tumor lobe.	$\kappa = 1.000$
Nodules in nontumor lobes	Presence of noncalcified nodule suspected to be malignant or indeterminate in the nontumor lobe.	$\kappa = 1.000$
Calcification	Presence of calcification in the tumor.	$\kappa = 0.866$
Lymphadenopathy	Thoracic lymph nodes (hilar or mediastinal) with short-axis diameter greater than 1 cm or with features suspicious for malignancy (heterogeneous, necrotic, invasive).	$\kappa = 1.000$
Pleural effusion and nodularity	Effusion and or nodularity of the ipsilateral or contralateral pleura.	$\kappa = 1.000$
Extrathoracic metastasis	Presence of extrathoracic tumor based on available imaging reports (eg, CT abdomen, PET/CT, or bone scan reports).	$\kappa = 1.000$

Abbreviations: CT, computed tomography; ICC, intraclass correlation; PET, positron computed tomography.

chest were obtained using one of the following CT scanners: Lightspeed VCT 64-slice or 16-slice CT scanners (GE Medical Systems, Chicago, Illinois), Revolution 64-slice CT scanner (GE Medical Systems, Chicago, Illinois), Ingenuity 64-slice CT scanner (Philips, Andover, Massachusetts), and Somatom 128-slice CT scanner (Siemens, Malvern, Pennsylvania).

The CT chest protocols were as follows: Nonenhanced scans were performed with tube voltage of 120 kVp, automatic-variable tube current, and image reconstruction at slice thickness of 1.25 mm, 3 mm, and 5 mm with multiplanar reformations. Intravenous contrast-enhanced scans with tube voltage of 120 kVp, automatic-variable tube current, image reconstruction at slice thickness of 1.25 mm, 3 mm, and 5 mm with multiplanar reformations were obtained with a 50-second delay following intravenous (IV) administration of 80 to 100 mL of iodinated contrast. Pulmonary CT angiography scans with tube voltage of 120 kVp, automatic-variable tube current, and image reconstruction at 1.25-mm thickness with multiplanar reformations were obtained with a variable delay following administration of 65 to 100 mL of IV contrast, based on the smart prep protocol or test bolus protocol. Nonionic iodinated contrast material (300 mg of iodine/mL, Omnipaque 300 mg/mL; GE Healthcare, Chicago, Illinois) was used for the contrast-enhanced studies.

Histopathology Protocol and EGFR Mutation Analysis

Lung cancer was classified according to the International Association for the Study of Lung Cancer/American Thoracic Society/European Respiratory Society 2011 system.[7] The EGFR mutation status was determined using the *EGFR* Mutation Analysis PCR assay (exons 18-20; EntroGen, Inc, Los Angeles, California) or TruSight Tumor 15 next-generation sequencing panel (exons 18-21; Illumina Inc, San Diego, California).

Data Interpretation

Two fellowship-trained thoracic radiologists with 5 and 7 years of experience in CT imaging of thoracic malignancies

Table 2. Descriptive Characteristics of Demographic Characteristics and CT-Derived Radiological Features by EGFR Status.

	Overall, n = 223	EGFR Negative, n = 111	EGFR Positive, n = 112	*P* Value
Age				
Mean (standard deviation)	67.5 (10.4)	67.7 (9.2)	67.2 (11.5)	.679
Gender				
Female (%)	126 (56.5)	54 (48.6)	72 (64.3)	.026
Male (%)	97 (43.5)	57 (51.4)	40 (35.7)	
Smoking				
>20 packs per year (%)	100 (44.8)	83 (74.8)	17 (15.2)	<.001
<20 packs per year (%)	115 (51.6)	28 (25.2)	87 (77.7)	
Shape				.599
Round (%)	20 (9)	11 (9.9)	9 (8)	
Oval (%)	39 (17.5)	17 (15.3)	22 (19.6)	
Irregular (%)	160 (71.7)	83 (74.8)	77 (68.8)	
Lobulation				.310
Absent (%)	101 (45.3)	46 (41.4)	55 (49.1)	
Present (%)	118 (52.9)	65 (58.6)	53 (47.3)	
Borders				.186
Smoothly, well defined (%)	47 (21.1)	28 (25.2)	19 (17)	
Ill defined (%)	161 (72.2)	74 (66.7)	87 (77.7)	
Obscured (%)	15 (6.7)	9 (8.1)	6 (5.4)	
Spiculation				.048
None (%)	64 (28.7)	40 (36)	24 (21.4)	
Fine (%)	61 (27.4)	25 (22.5)	36 (32.1)	
Coarse (%)	93 (41.7)	45 (40.5)	48 (42.9)	
Texture				.734
Pure GGO or mixed attenuation (%)	35 (15.7)	16 (14.4)	19 (17)	
Solid (%)	188 (84.3)	95 (85.6)	93 (83)	
Air bronchogram				.798
Absent (%)	160 (71.7)	81 (73)	79 (70.5)	
Present (%)	63 (28.3)	30 (27)	33 (29.5)	
Air in tumor				.201
Absent (%)	194 (87)	93 (83.8)	101 (90.2)	
Bubbly-like (%)	17 (7.6)	12 (10.8)	5 (4.5)	
Cavitation (%)	12 (5.4)	6 (5.4)	6 (5.4)	
Calcification				1.000
Absent (%)	207 (92.8)	103 (92.8)	104 (92.9)	
Present (%)	16 (7.2)	8 (7.2)	8 (7.1)	
Retraction				.106
Absent (%)	66 (29.6)	39 (35.1)	27 (24.1)	
Present (%)	156 (70)	72 (64.9)	84 (75)	
Attachment				.304
Absent (%)	17 (7.6)	11 (9.9)	6 (5.4)	
Present (%)	206 (92.4)	100 (90.1)	106 (94.6)	
Emphysema				<.001
Absent (%)	148 (66.4)	49 (44.1)	99 (88.4)	
Present (%)	75 (33.6)	62 (55.9)	13 (11.6)	
Fibrosis				.474
Absent (%)	220 (98.7)	109 (98.2)	111 (99.1)	
Present (%)	1 (0.4)	0 (0)	1 (0.9)	
Long-axis size (cm)				
Mean (standard deviation)	3.8 (2.1)	4.2 (2.4)	3.4 (1.7)	.005
Short-axis size (cm)				
Mean (standard deviation)	3.1 (1.8)	3.4 (2)	2.8 (1.5)	.017
Distribution				
Central (%)	40 (17.9)	22 (19.8)	18 (16.1)	.372
Middle (%)	115 (51.6)	52 (46.8)	63 (56.2)	
Peripheral (%)	68 (30.5)	37 (33.3)	31 (27.7)	

(continued)

Table 2. (continued)

	Overall, n = 223	EGFR Negative, n = 111	EGFR Positive, n = 112	*P* Value
Lobe location				
Right upper lobe (%)	85 (38.1)	48 (43.2)	37 (43.2)	.527
Right middle lobe (%)	12 (5.4)	6 (5.4)	6 (5.4)	
Right lower lobe (%)	38 (17)	17 (15.3)	21 (15.3)	
Left upper lobe (%)	51 (22.9)	25 (22.5)	26 (22.5)	
Left lower lobe (%)	37 (16.6)	15 (13.5)	22 (13.5)	
Lymphadenopathy				
Absent (%)	90 (40.4)	37 (33.3)	53 (47.3)	.046
Present (%)	133 (59.6)	74 (66.7)	59 (52.7)	
Pleural effusion and nodularity				
Absent (%)	154 (69.1)	79 (71.2)	75 (67)	.70
Ipsilateral (%)	54 (24.2)	25 (22.5)	29 (25.9)	
Contralateral (%)	0	0	0	
Bilateral (%)	14 (6.3)	7 (6.3)	7 (6.2)	
Extrathoracic metastasis				
Absent (%)	81 (36.3)	39 (35.1)	42 (37.5)	1.000
Present (%)	133 (59.6)	65 (58.6)	68 (60.7)	
Nodules in primary tumor lobe				
Absent (%)	93 (41.7)	40 (36)	53 (47.3)	.115
Present (%)	130 (58.3)	71 (64)	59 (52.7)	
Nodules in nontumor lobe				
Absent (%)	74 (33.2)	36 (32.4)	38 (33.9)	.924
Present (%)	149 (66.8)	75 (67.6)	74 (66.1)	

Abbreviations: CT, computed tomography; EPFR, epidermal growth factor receptor; GGO, ground glass.

independently assessed the CT images, following a standardized reporting scheme. Both readers received a study list in Microsoft Excel file that included an anonymized list of CT examinations, including a specific identification number for each CT scan and CT features as detailed in Table 1. Computed tomography images were accessed using hospitals picture archiving and communication systems.

At the time of CT scan assessment, both readers were blinded to the patient's demographic data, smoking status, tumor stage, and EGFR mutation analysis results. In the event of interobserver disagreement, discrepant cases were reevaluated by the readers until a consensus was reached.

Statistical Analysis

Descriptive statistics were used to analyze patient's clinical information and radiological features collected postconsensus. The statistics were presented for both the overall cohort and subcohorts stratified by EGFR mutation status. For categorical variables, cross-tabulations of frequencies were determined and a χ^2 test was applied to test whether there were significant differences in distribution between different EGFR mutation status groups. For continuous variables, mean and standard deviation were determined and a 2-sampled *t* test was used to test whether there was a significant difference in mean between the different EGFR mutation status groups. In addition, inter-reader agreement between the readers was determined using intraclass correlation for continuous variables and Cohen κ for categorical variables.[8,9] Because of the exploratory nature of this study, all hypothesis testing was done at $\alpha = .05$ level and not adjusted for multiple hypothesis testing.

For multivariate analyses, logistic regression models were created for each radiological feature, using EGFR status as a binary outcome, and adjusted for age, sex, and smoking status as confounders. Odds ratios were determined for each radiological feature from their respective logistic regression along with its associated 95% confidence interval (CI) and *P* value.

Finally, to visualize and interpret the added discriminant ability of radiological features of NSCLC to predict EGFR status, 2 multivariate logistic regression models were generated based on backward model selection under the assumption that radiological features provide added benefit as predictors of EGFR status. The first logistic regression model was created using clinical variables only, and the second model was created using clinical variables in addition to radiological features variables. Receiver operating characteristic (ROC) curves along with their associated areas under of the curve (AUCs) were generated.

Results

Most of the patient population were Caucasian in their background 89% (217/223), while 11% (26/223) were Asian in origin in both groups. Of these Asian, 21 of 26 had EGFR mutation. The mean age of the 111 patients with EGFR mutation-negative tumors was 67.7 years and did not significantly differ from mean age of the 112 patients with EGFR mutation-positive tumors (67.2 years; $P = .679$). The EGFR mutation-positive tumors were significantly more common in

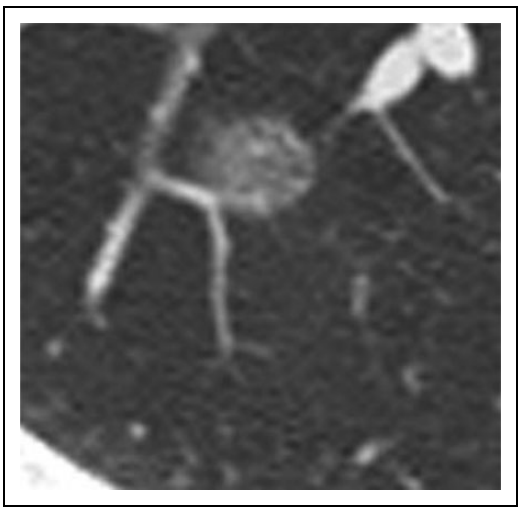

Figure 1. Axial computed tomography scan of the chest in lung window demonstrating a well-defined, oval-shaped, ground-glass nodule. There are no spiculations, lobulations, or air bronchograms.

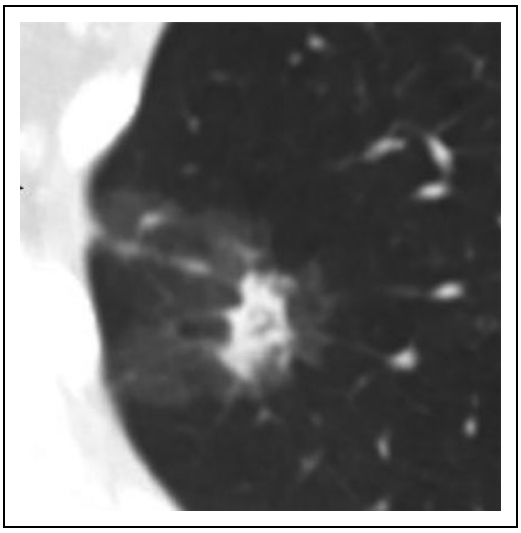

Figure 2. Axial computed tomography scan of the chest obtained in lung window demonstrating part solid and part ground-glass irregular nodule with ill-defined borders and coarse spiculations.

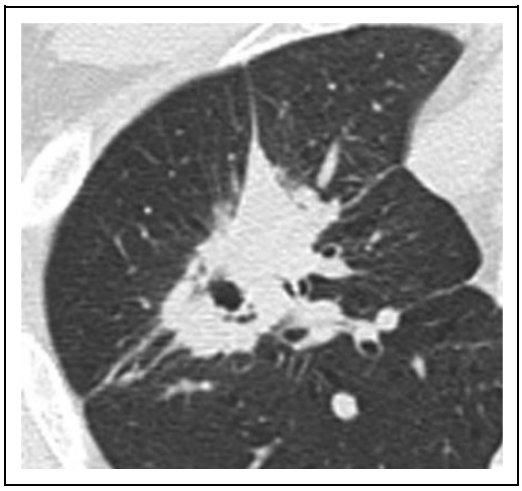

Figure 3. Axial computed tomography scan of the chest obtained in lung window demonstrating large irregular mass with central cavitation, coarse spiculations, and subtle pleural retraction.

Figure 4. Axial computed tomography scan of the chest obtained in lung window demonstrating large irregular mass with lobulation, air bronchogram, internal cavitation, and pleural attachment. Figure 5.

female patients (72/126, 57%) than in male patients (40/97, 41%; $P = .026$). Of the 115 patients who had less than 20 pack-year smoking history, 87 (78%) had EGFR mutation-positive tumors, which is significantly higher than in those with more than 20 pack-year smoking history (17/100, 17%; $P < .001$). Demographic characteristics of our study population can be found in Table 2.

Detailed definitions of each radiological feature analyzed in this study along with the inter-reader agreement are presented in Table 1 and Figures 1 to 4. There was a high inter-reader agreement for all categorical variables, as well as very high inter-reader agreement for continuous variables. There was an almost perfect inter-reader agreement for the presence/absence of emphysema (κ value of .897) and calcification (.866). There was a substantial inter-reader agreement for texture (.795), lobulation (.766), air bronchogram (.728), borders (.697), air within tumor (.677), and pleural or fissural retraction (.627).

Descriptive statistics of radiological features are presented in Table 2. Of the radiological features examined in this study, long and short diameters ($P = .005$ and $P = .017$, respectively), the presence of emphysema ($P < .001$), the presence of lymphadenopathy ($P = .046$), and spiculation ($P = .048$) showed statistically significant differences in distribution between EGFR mutation-negative and EGFR mutation-positive patients.

The odds ratios for each radiological feature from logistic regression adjusting for age, sex, and smoking status are presented in Table 3. The odds of EGFR-activating mutation were found to be higher when tumors demonstrate fine spiculations (odds ratio,

Table 3. Odds Ratios of CT Radiological Features From Logistic Regressions Fitting Each Radiological Feature Individually Adjusting for Age, Gender, and Smoking Status.[a,b]

	Odds Ratio	2.5%	97.5%	*P* Value
Shape				
Round	Reference	–	–	–
Oval	1.917	0.513	7.265	.333
Irregular	1.425	0.461	4.399	.535
Lobulation				
Absent	Reference	–	–	–
Present	0.97	0.497	1.906	.928
Borders				
Smoothly, well defined	Reference	–	–	–
Ill defined	2.191	0.949	5.2	.069
Obscured	0.906	0.208	3.911	.894
Spiculation				
None	Reference	–	–	–
Fine	3.834	1.525	10.19	.005
Coarse	2.395	1.06	5.58	.038
Texture				
Pure GGO or mixed attenuation	Reference	–	–	–
Solid	1.196	0.466	3.042	.707
Air bronchogram				
Absent	Reference	–	–	–
Present	1.071	0.508	2.278	.856
Air in tumor				
Absent	Reference	–	–	–
Bubbly-like	0.369	0.084	1.412	.158
Cavitation	1.739	0.414	7.196	.442
Calcification				
Absent	Reference	–	–	–
Present	1.260	0.352	4.594	.723
Retraction				
Absent	Reference	–	–	–
Present	1.787	0.865	3.753	.119
Attachment				
Absent	Reference	–	–	–
Present	2.913	0.868	10.263	.086
Emphysema				
Absent	Reference	–	–	–
Present	0.192	0.077	0.451	<.001
Distribution				
Central	Reference	–	–	–
Middle	1.266	0.504	3.182	.614
Peripheral	0.871	0.319	2.36	.785
Long-axis size	0.850	0.72	0.998	.05
Short-axis size	0.833	0.686	1.005	.058
Lymphadenopathy				
Absent	Reference	–	–	–
Present	0.596	0.294	1.189	.144
Pleural effusion and nodularity				
Absent	Reference	–	–	–
Ipsilateral	1.216	0.55	2.71	.629
Bilateral	0.499	0.139	1.848	.285
Extrathoracic metastasis				
Absent	Reference	–	–	–
Present	0.806	0.386	1.652	.559
Nodules in primary tumor lobe				
Absent	Reference	–	–	–
Present	0.996	0.478	2.07	.991
Nodules in nontumor lobe				
Absent	Reference	–	–	–
Present	0.728	0.358	1.47	.375

Abbreviations: CT, computed tomography; EPFR, epidermal growth factor receptor; GGO, ground glass.
[a]An odds ratio >1 suggests a tumor is more likely to be EGFR positive.
[b]The features of fibrosis and lobe location are excluded from this analysis due to distribution issues.

3.834; 95% CI, 1.525-10.19) or coarse spiculations (odds ratio, 2.395; 95% CI, 1.06-5.58), and lower when tumors are of large size (odds ratio, 0.850; 95% CI, 0.72-0.998) or are associated with emphysema (odds ratio, 0.192; 95% CI, 0.077-0.451).

Using a backward model selection, the selected model with only clinical variables included smoking status as predictors of EGFR status as covariates, and the selected model with both clinical and radiological features included smoking status, small tumor diameter, fine and coarse spiculations, noncentral location, and the absence of diffuse emphysema and pleural attachments as covariates. The details of the multivariate model are presented in Table 4. The ROC curve depicting the discriminant ability of these 2 models is shown in Figures 5. The area under the curve of the ROC curves (AUC) demonstrates an increase in the discriminant ability from 0.788 to 0.879 when radiological features are included in the analysis in addition to clinical features.

Discussion

A subset of NCSLC is known to express activating mutation in the *EGFR* gene. Detection of such mutation in a tumor is important because (1) targeted TKI therapy exists specifically for these types of cancers and (2) such therapy has been associated with improved response rate, disease control, and patient's quality of life.[10] Histopathological confirmation of EGFR-activating mutation is currently required for selecting patients for treatment with TKI. However, on occasion, adequate tissue samples cannot be safely and/or efficiently obtained. In these situations, accurate clinical–radiological tools would be of benefit in predicting the presence of EFGR-activating mutation in targeted tumors.

Several studies previously described correlations between CT features of lung adenocarcinomas and EGFR mutations. For example, Liu et al[5] examined 385 surgically resected lung adenocarcinomas in a Chinese population and found that EGFR mutations were more frequent in females, never smokers, and associated with lesions of smaller size, ground-glass or mixed attenuation, partially defined borders, spiculated margins,

Table 4. Summary of Multivariable Logistic Regressions for Clinical Only and Clinical + Radiological Model Selected by Stepwise Model Selection.

	Odds Ratio[a]	2.5%	97.5%	*P* Value
Clinical model (AUC = 0.788)				
Smoking				
>20 packs per year	Reference	–	–	–
<20 packs per year	14.298	7.438	28.844	<.001
Clinical + radiological feature model (AUC = 0.879)				
Smoking				
>20 packs per year	Reference	–	–	–
<20 packs per year	9.263	4.222	21.386	<.001
Long-axis size	0.834	0.681	1.012	.069
Spiculation				
None	Reference	–	–	–
Fine	3.793	1.393	10.861	.005
Coarse	2.157	0.883	5.417	.095
Attachment				
Absent	Reference	–	–	–
Present	3.641	0.915	15.318	.070
Emphysema				
Absent	Reference	–	–	–
Present	0.169	0.064	0.416	<.001
Distribution				
Central	Reference	–	–	–
Middle	0.922	0.310	2.718	.882
Peripheral	0.451	0.138	1.428	.180

Abbreviations: AUC, area under of the curve; EPFR, epidermal growth factor receptor.
[a]An odds ratio greater 1 suggests a tumor is more likely to be EGFR positive.

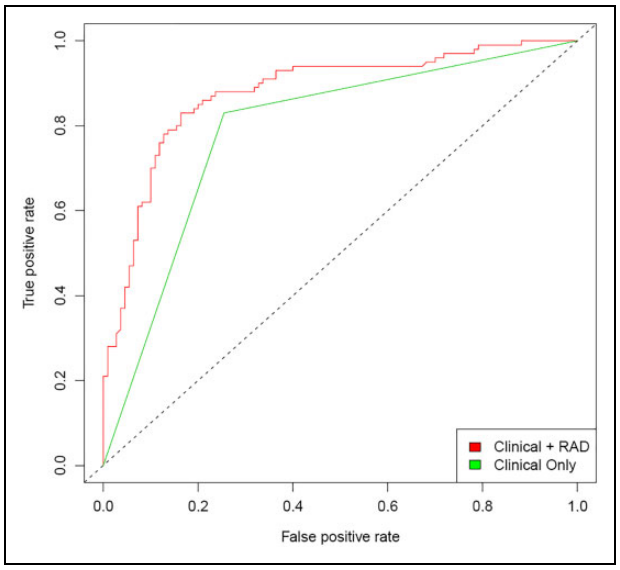

Figure 5. Summary of the area under the ROC curve using clinical variable versus clinical + radiological model.

containing air bronchogram and bubble-like lucency, and with absence of severe emphysema, pleural retraction, and lymphadenopathy. In another study, Choi et al[11] examined 130 patients of Asian ethnicity with stage IV lung adenocarcinoma and found association between EGFR mutation and female sex, never-smoker status, smaller lesions, lesions with ground-glass texture, spiculated margins, and cavitation. Finally, Rizzo et al[12] examined 64 patients in an Italian population and found EGFR mutation association with female sex, never-smoker status, small lesion size, ground-glass opacity, irregular borders, spiculated margin, air bronchograms, and lack of bubble-like lucency, emphysema, fibrosis, and pleural retraction.

In our study of a multiethnic Canadian population, we noted that adenocarcinomas of the lung tend to be solid, irregular, and with ill-defined borders. Lung adenocarcinomas with EGFR-activating mutation were significantly more common in women and in patients with less than 20 pack-year history of smoking, which is consistent with previously published data. In our study, we also examined the relationship between 20 CT features of adenocarcinomas of the lung and their EGFR mutation status. From a radiological perspective, we found that tumors of smaller size, with fine or coarse spiculations, in the absence of emphysema and lymphadenopathy, were significantly more likely to express EGFR mutation. These CT features are concordant with characteristics that were previously described in published studies assessing Asian population.

All other radiological features that were previously described to be significantly more present in EGFR mutation-positive adenocarcinomas did not meet criteria for significance in our study; however, these demonstrated tendency to be more common in EGFR mutation-positive tumors (Table 4).[5,11] Although focal or diffuse fibrosis was not frequent in EGFR mutation-positive cases in both Asian and Canadian cohorts, we noted that fibrosis was more frequent in Liu et al's[5] study (36.3%) compared to a single case (0.9%) in our study.

To the best of our knowledge, this is the first study to examine the correlation between radiological features and EGFR mutation status in NSCLC in a North American population. Identification of CT findings that are specific to EGFR-positive adenocarcinomas could have an impact on the way lung cancer tumors are radiologically classified. If validated, use of imaging and clinical features as surrogate markers for EGFR mutation could potentially decrease the need for additional and often invasive procedures in order to obtain tumor tissue for molecular testing, which would particularly be beneficial for centers where such procedures and/or molecular testing are not readily available. It could also reduce time to initiation of targeted therapy with TKI regiments. Finally, one would further expect improvement in cost-efficiency and decrease in financial burden on health systems.

The current study is invariably limited by its retrospective nature. As well, our patient selection was based on a sample of convenience. Thus, it is possible that unmeasured confounders have occurred during patient selection. Furthermore, our study included lung adenocarcinomas of early and late stages, which theoretically may have prevented detection of true morphological differences between tumors of different EGFR mutation status. Finally, although this study assessed most of the imaging features previously described,[5] a few features such as

vascular convergence and tumor enhancement were not examined in our study due to different study protocols. Larger studies may reveal more important correlation between CT features of lung adenocarcinomas and EGFR mutation status and improve their positive predictive value.

Conclusion

Our findings suggest that EGFR mutation-positive lung adenocarcinomas in a Canadian population, mainly Caucasian, are more likely to be present in women, in patients with no-history or mild-history of smoking, in tumors of smaller size with fine or coarse spiculations, in the absence of emphysema and lymphadenopathy, which is similar to findings described in prior studies of Asian population. Our study further provides support to the belief that imaging features of NSCLC derived from CT scans may serve as surrogate markers for EGFR mutation status in NSCLC and improve predictive ability of EGFR mutation status when used in conjunction with clinical variables.

Declaration of Conflicting Interests

The author(s) declared no potential conflicts of interest with respect to the research, authorship, and/or publication of this article.

Funding

The author(s) received no financial support for the research, authorship, and/or publication of this article.

References

1. Carbonnaux M, Souquet PJ, Meert AP, Scherpereel A, Peters M, Couraud S. Inequalities in lung cancer: a world of EGFR. *Eur Respir J*. 2016;47(5):1502-1509.
2. Dela Cruz CS, Tanoue LT, Matthay RA. Lung cancer: epidemiology, etiology, and prevention. *Clin Chest Med*. 2011;32(4): 605-644.
3. Díaz-Serrano A, Gella P, Jiménez E, Zugazagoitia J, Paz-Ares Rodríguez L. Targeting EGFR in lung cancer: current standards and developments. *Drugs*. 2018;78(9):893-911.
4. Kwapisz D.The first liquid biopsy test approved. Is it a new era of mutation testing for non-small cell lung cancer? *Ann Trans Med*. 2017;5(3):46.
5. Liu Y, Kim J, Qu F, et al. CT features associated with epidermal growth factor receptor mutation status in patients with lung adenocarcinoma. *Radiology*. 2016;280(1):271-280.
6. Shigematsu H, Lin L, Takahashi T, et al. Clinical and biological features associated with epidermal growth factor receptor gene mutations in lung cancers. *J Natl Cancer Inst*. 2005;97(5): 339-346.
7. Travis WD, Brambilla E, Noguchi M, et al. International Association for the Study of Lung Cancer/American Thoracic Society/European Respiratory Society International Multidisciplinary Classification of Lung Adenocarcinoma. *J Thorac Oncol*. 2011;6(2):244-285.
8. McHugh ML. Interrater reliability: the kappa statistic. *Biochem Med*. 2012;22(3):276-282.
9. Koo TK, Li MY. A guideline of selecting and reporting intraclass correlation coefficients for reliability research. *J Chiroprac Med*. 2016;15(2):155-163.
10. Rosell R, Carcereny E, Gervais R, et al. Erlotinib versus standard chemotherapy as first-line treatment for European patients with advanced EGFR mutation-positive non-small-cell lung cancer (EURTAC): a multicentre, open-label, randomised phase 3 trial. *Lancet Oncol*. 2012;13(3):239-246.
11. Choi CM, Kim MY, Hwang HJ, Lee JB, Kim WS. Advanced adenocarcinoma of the lung: comparison of CT characteristics of patients with anaplastic lymphoma kinase gene rearrangement and those with epidermal growth factor receptor mutation. *Radiology*. 2015;275(1):272-279.
12. Rizzo S, Petrella F, Buscarino V, et al. CT radiogenomic characterization of EGFR, K-RAS, and ALK mutations in non-small cell lung cancer. *Eur Radiol*. 2016;26(1):32-42.